Morphogenesis of Silicovanadate Glasses: Investigation of Physical Properties

Md. Moinul lslam[1], Md. Abdur Rashid[1], Md. Parvez Ahamed[1], Md. Emran Hossain[2], M. Rafiqul Ahsan[1], M. Golam Mortuza[1], Mirza Humaun Kabir Rubel[3, *

[1]Department of Physics, University of Rajshahi, Rajshahi–6205, Bangladesh
[2]Physics Discipline, University of Khulna, Khulna–9208, Bangladesh
[3]Department of Materials Science and Engineering, University of Rajshahi, Rajshahi–6205, Bangladesh

ABSTRACT

In this article, we demonstrate the synthesis and various characterizations of silicovanadate glasses of $xSiO_2$ $(100-x)V_2O_5$ for $x = (10-50)$ mol%, glasses which are prepared by the melt quenching method. FTIR spectra analysis confirms dominant chemical bonds among silicon, vanadium, and oxygen elements as expected. The assigned chemical bonds are Si-O-Si, O-Si-O, V-O-V, V=O, Si-O-V, O-H from FTIR spectra. The IR spectra of all glass specimens were baseline corrected and deconvoluted to distinct peaks of chemical bonds in overlapped Gaussians with employing computer program. The chemical bond's position shifted and affected due to the addition of vanadium pentaoxide by the heat treatment process. The X-ray diffractions (XRD) patterns of glass samples exhibit partial crystalline nature for 10S90V and 50S50V that is influenced by high-temperature application. The differential thermal analysis (DTA) of base and heat-treated specimen determines the glass transition (T_g), crystallization, and liquidus temperature with prominent exothermic and endothermic reactions. It is seen that the pH of the glass specimens abruptly changes due to the surface effect of V_2O_5 while bulk effects become robust after about 30 minutes. The measured hardness of three glass samples shows high H_V-values and a slight linear increment is observed for higher V_2O_5 contents. The current-voltage (I-V) characteristic connected to the electrical conductivity of the glass specimen (20S80V) shows a relatively higher and non-linear trend of conductivity which reveals the behavior of a semiconductor. Moreover, temperature-dependent electrical resistivity measurement of the same sample (20S80V) manifests the semiconducting nature up to 427 °C as well.

Keywords: Si/V-based glass, FTIR, X-ray diffraction, DTA, pH, Current-Voltage characteristics, Electrical resistivity.

1 Introduction

Glass-ceramics are polycrystalline or amorphous substances possessing the properties of hardness, rigidity, brittleness which are prepared by controlled crystallization processes. Glass ceramics have widespread attentive technological applications in various fields such as electronic devices, optical devices, reflecting windows, ray absorbers, mechanical sensors, electro-optic devices, sealants, etc. [1]-[4]. Among various oxides glasses, the silicovanadate glasses have great scientific vast technological, and attractive industrial interest for their individual characteristics. To know the structural information, electrical conductivity, hardness, solubility, and optical properties of this silicovanadate glasses various characterization techniques such as X-ray diffraction, Fourier Transform IR study, Four probe method, Vickers hardness testing system, pH meter [5]-[8], etc., have been utilized where vanadium metal manifests various physical and chemical properties. However, some oxide glasses are generally insulating type in the aspect of conductivity but the addition of some transition metal such as VO, V_2O_5, Fe_2O_3, WO_3, ZnO, etc. make these glasses semiconducting.

These binary oxide glasses are studied widely for their attractive potential applications in various fields such as optical and electrical memory switching, solid state devices, and optical fibers [9]. For making useful memory and switching devices in various fields V_2O_5 containing glasses are extensively used for its transition behavior. In order to get silicovanadate glasses,

V_2O_5 is used among various transition metals because of having electrical conductivity due to the electron hopping behavior between V^{5+} and V^{4+} ions [10]-[13]. In this $xSiO_2(100-x)V_2O_5$ binary system glasses, Si^{4+} ions act as network forming ions whereas vanadium ions might act diverse role either as network formers, modifiers, and/or intermediate in the amorphous glass network [14]. The most important property of the glassy materials is the viscosity which makes the glass in liquid nature and is also closely connected with the nature and structure of the melts [15]-[16]. Besides, the addition of the network modifier component in the composition increases the density as the network modifier ions attempt to occupy the interstices within the network. Noteworthy, the hardness of glasses makes strength and density of packing of the atoms in the localized structure [17]. During the course of this investigation, the microhardness (GPa) of silicate-based glasses has been studied to investigate mechanical performance on the basis of well-established factors [18]-[22]. The electrical conductivity of a glass system usually changes due to the presence of network modifiers [14]. V_2O_5 exhibits semi-conductivity for the presence of V^{5+} and V^{4+} oxidation states that originate electron hopping between these two ions [23]-[24]. Recently, the electrical properties of several new V/Fe-based glasses have been analyzed to relate the structure and electrical conductivity (σ) for their important applications [25]-[30]. Moreover, the chemical durability and possible improvement of the aforementioned glasses with electrical conductivity have also been analyzed [25]. Following this, the solubility of our prepared glasses in air condition has

been measured by means of pH meter to explore physio-chemical changes in the specimens. Therefore, in this article, we have prepared and established a relationship between local structure and physical properties such as electrical conductivity, hardness, thermal behavior, and solubility of several silicovanadate glasses by FTIR, XRD, four-probe method, DTA, TCR, and pH meter for the first time.

2 Materials and Methods

For the synthesis of silicovanadate glasses by the conventional melt quenching method, commercially available reagents SiO_2 and V_2O_5 were chosen as starting compositions. The chemicals Vanadium oxide (V_2O_5) and Silica (SiO_2) were collected from Merck Specialties Pvt. Ltd. Worli, Mumbai-400018. These chemicals were used directly without any further purification. For the preparation of 20 gm batch of $xSiO_2(100-x)V_2O_5$ glass system the collected raw materials were homogeneously mixed both in an agate mortar and ball-milled machine for 6-8 hours. The mixture was then poured into a porcelain crucible and melted in an electric carbolite furnace at ~1500 °C for 1 hour. Dull brown transparent glass specimens were observed after sudden quenching using steel block and hammer assembly. Afterward, the base glass samples were placed in an Aluminum crucible and heated at 500 °C/1h to study the differences in physical properties post heat treatment.

FTIR spectra of the silicate vanadate glasses were collected on a Spectrum 100, Perkin Elmer spectrophotometer by KBr disk method within the wavenumber of 400 and 4000 cm^{-1} to know all possible chemical bonds. X-ray diffraction patterns of base and heat-treated glasses were examined using the monochromatic CuK$_\alpha$ radiation by setting 2θ in the range of 5° to 50° at a scanning rate of 0.02° with Philips "X-pert Pro XRD system". Crystal phases were detected based on standards compiled by the International Center for Diffraction Data (ICDD). The important phase transformations and crystallization temperatures were investigated by a STA-8000 DTA model (Parkin Elmer) meter as well. Differential thermal analysis (DTA) was carried out from room temperature (RT) to 900 °C by varying the heating rate from 5 to 10 °C min^{-1}. During the measurement, about ten milligrams of α-Al_2O_3 powder and finely pulverized glass were utilized as a reference sample. To investigate physical and chemical changes the solubility of the glass specimens is measured with the aid of a pH/mv meter (Model-PHS-25, China). In this experiment, the scale of the meter was calibrated using Potassium hydrogen phthalate of (pH = 4.0) and the Sodium tetraborate of (pH = 9.18) to read pH directly. Temperature-dependent electrical conductivity (σ) and resistivity (ρ) were carried out by employing dc four-probe method for 20S80V glass specimen only. The glass specimen was cut into a rectangular shape and each longitudinal edge was connected by the probe(s) using Ag solder. The electrical current (I) was recorded through alternating voltage between 1.0 and 15 V, on the other hand, the voltage (V) was registered by changing electrical current between 1.0 and 2.0 mA along both length and width direction. Moreover, the electrical conductivity(σ) of glass sample was evaluated on the basis of the following equation: $\sigma = R^{-1}\cdot S^{-1}\cdot l$; where R, S, and l are electrical resistivity (Ω) estimated from a slope of the straight line of V vs. I, surface area (cm^2) and electrode distance (cm), respectively.

The microhardness of the prepared glasses was as curtained by Vickers indentation (Matsuzawa microhardness tester (MXT-α1) equipped with a pyramidal diamond indenter under (100 g

load, 20 s) by neglecting the size effects of indentation [17],[26]-[27]. The H_V-values (GPa) of glass samples were calculated from the expression as given, $H_V = 1854F/d^2$, here F = 9.81 N, and d is the average indentation diagonal in μm, as reported elsewhere [26]. The values are recorded on averages over 8–10 independent measurements. The indentations were examined and evaluated via the attached high-resolution microscope.
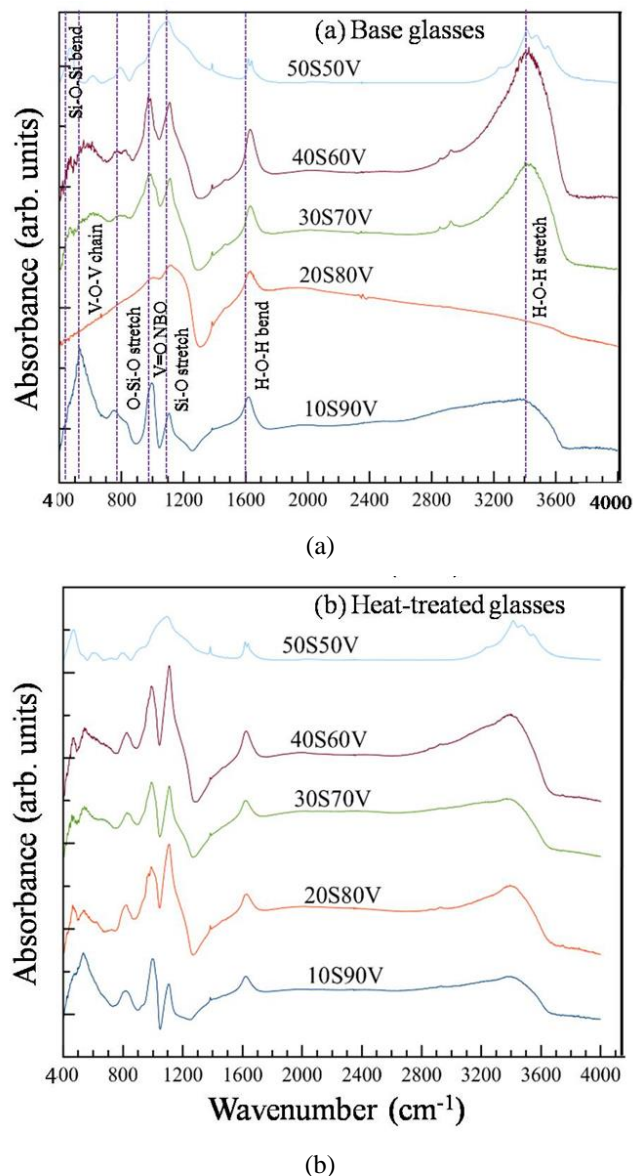

(a)

(b)

Fig. 1 Infrared spectra of (a) base glass and (b) heat-treated glass samples.

3 Results and Discussion

3.1 FTIR Analysis of Silicovanadate Glasses

Fourier Transform Infrared (FTIR) absorption spectra of glasses usually provide significant and valuable information on the arrangement of atoms, the chemical bonding between them, and the changes in atomic configurations caused by the increase or decrease of concentration of glass-forming systems. FTIR absorbance spectra of different silicate vanadate glasses are recorded from 400 cm^{-1} to 4000 cm^{-1} at room temperature. Fig. 1 (a) and 1(b) show FTIR spectra of $xSiO_2(100-x)V_2O_5$ of base glass and heat-treated glass samples respectively, with assigned prominent bonds and added vanadium pentaoxide contents. The

interpretation of the IR-spectra is based on the literature data of a series of crystalline and amorphous vanadate phases [29]-[34]. The Structural groups are assigned respectively, Si-O-Si bonds for bending vibration in 458-466 cm^{-1} [35]-[37], V-O-V bonds for chain vibration in 512-552 cm^{-1} [38]-[41].

V-O-V bonds for bending vibration in 593-624 cm^{-1} [42], O-Si-O bonds for symmetric stretching vibration in 798 cm^{-1} [43], V-O-V bonds for asymmetric stretching vibration in 822-826 cm[-1][44], Si-O-V bonds for vibration in 911 cm^{-1} [45], V=O bonds for non-bridging in 980-998 cm^{-1} [46], Si-O-Si bonds for asymmetric stretching vibration in 1073 cm^{-1} [47], Si-O bonds for asymmetric stretching vibration in 1104-1227 cm^{-1} [48]-[50]. Whereas, O-H bonds for vibration in 1385-1523 cm^{-1} [51], H-O-H bonds for bending vibration in 1601-2028 cm^{-1} [52]-[56], H-O-H bonds for symmetric stretching vibration in 3403-3447 cm^{-1} [57]-[58] for hygroscopic nature. However, we did not observe any significant change in the FTIR spectra of our synthesized glass samples even after heat treatment. The structural groups and main bonds of heat-treated samples remain in almost harmonious peak positions like base glasses, except a slight change in their intensity. This means that the local structure of the synthesized glass specimens did not alter after heat treatment up to 500 °C. Table 1 displays several physical properties

including melting temperature during synthesis of all glasses. However, the melting temperature of 50S50V sample was undetermined or known due to a large amount of silica (melting temperature ~1700 °C) present.

Table 1 Melting temperature and optical quality of the glasses of various compositions.

Samples	Nominal composition (mol %)		Melting Temperature (ºC)	Optical quality	X-ray diffraction
	Si₂O	V₂O₅			
10S90V	10	90	1200	Transparent	Partially Crystallized
20S80V	20	80	1250	Transparent	Amorphous
30S70V	30	70	1300	Transparent	Amorphous
40S60V	40	60	1300	Transparent	Amorphous
50S50V	50	50	Unknown	Opaque	Amorphous

Table 2 Deconvoluted band positions of $xSiO_2(100-x)V_2O_5$ base and (heat-treated) glasses.

Chemical Bonds	Band position (cm⁻¹)				
	10S90V	20S80V	30S70V	40S60V	50S50V
Si-O-Si (Bending)	466 (480)	- (463)	458 (458)	464 (462)	466 (467)
V-O-V (Chain)	528 (543)	- (532)	512 (536)	552 (539)	- (-)
V-O-V (Bending vibration)	593 (601)	- (591)	602 (632)	624 (602)	616 (610)
V-O (stretching Vibration)	763 (-)	736 (-)	- (-)	784 (-)	749 (728)
O-Si-O (symmetric Stretching Vibration)	- (-)	- (-)	- (-)	- (-)	798 (799)
V-O-V (Asymmetric Vibration)	826 (820)	- (815)	822 (830)	- (824)	- (-)
Si-O-V (Vibration)	- -	- -	- -	- -	911 (921)
V=O (Non bridging)	991 (987,1011)	998 (972,1007)	991 (953,997)	980 (948,992)	- (1002)
Si-O-Si (Asymmetric Stretching Vibration)	- (-)	- (-)	- (-)	- (-)	1073 (1088)
Si-O (Asymmetric Stretching Vibration)	1105,1168 (1103,1157)	1137,1212 (1100,1127, 1196)	1112,1174 (1107,1172)	1104,1192 (1105,1182)	1227 (1212,1261)
O-H (vibration)	1390,1523 (1400,1572)	1470 (1380,1503)	1441 (1405,1535)	1385,1512 (1415,1519)	- (-)
H-O-H (Bending vibration)	1619 (1630)	1616,1752, 2028 (1629)	1601,1633 (1628)	1632 (1627)	1635 (1618,1637)

In order to obtain the quantitative information, the spectra of the base and heat-treated glasses are deconvoluted to several Gaussians according to the presence of peaks and shoulders in the spectral shape. The high-frequency band peaks have a relatively higher intensity than low-frequency band peaks and consist of broad Gaussian. The shape of the absorption spectrum changes with increasing V_2O_5 content up to 90 mol%.

The structural bonds of base samples slightly shift in contrast to heat-treated samples. The FTIR spectra are divided into two regions, one in the lower wavenumber from 400 cm^{-1} to 1700 cm^{-1} and the other in the higher frequency range 1700 cm^{-1}-4000 cm^{-1}. As it is difficult to identify the exact position of the absorption band thus deconvolution of these bands was carried out to obtain the exact position of the absorption band [28]. The

deconvolution of 10S90V, 20S80V, 30S70V, 40S60V, and 15S50V base and heat-treated glasses with baseline correction are shown in Fig. A1.

The spectra exhibited different absorption bands due to various structural units of SiO_2 and V_2O_5. Further, the deconvolution method also can calculate the relative area of each component band and band positions of base and heat-treated glasses (Fig. A2). The concentration of the structural group is proportional to the relative area of its component bands. The summary of the data on various absorption bands observed in the deconvolution IR spectra of $xSiO_2(100-x)V_2O_5$ of base and heat-treated glasses are presented in the values within (heat-treated) are indicated for heat-treated glasses.
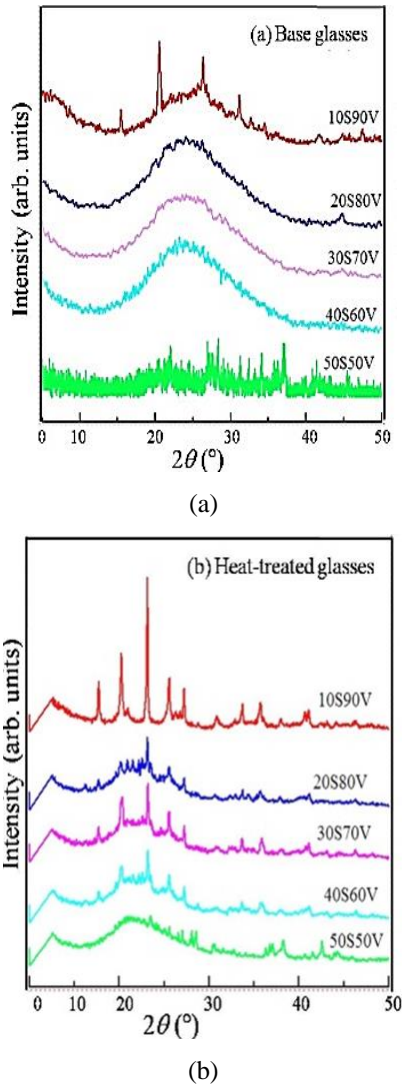

(a)

(b)

Fig. 2 The X-ray diffraction patterns of (a) base and (b) heat-treated glass samples.

3.2 XRD analysis of silicovanadate glasses

To know the crystalline nature of the prepared base and heat-treated glass samples X-ray diffraction patterns were collected and analyzed, which are shown in Fig. 2. The XRD patterns of base glass samples are shown in Fig. 2(a). All the base glass samples display weak diffuse diffraction patterns with amorphous halos except 10S90V composition. The sample 10S90V is partially crystallized because some peaks are observed at about 15°, 20°, 28°, 32° due to the formation of

several phases of silicovanadate compounds. However, few weak diffuse halos are observed in the 20S80V, 30S70V, 40S60V, and 50S50V base glasses that imply the homogeneous nature of prepared glasses. Moreover, the XRD patterns of heat-treated glass samples are cumulated and shown in Fig. 2(b).

X-ray diffraction study of heat-treated glass samples shows the formation of possible primary crystalline phases of SiV_2O_7, $Si_2V_2O_6$, and $Si_2V_2O_9$ indicating the multiple combinations of elements [45]. The exact peak positions corresponding to phases of heat-treated glasses were not determined for the limited feature of the XRD machine. From X-ray diffraction patterns it is seen, the crystalline peak increases with increasing V_2O_5 contents in the case of heat-treated glass samples. Therefore, phase formation in our synthesized base glasses depends both on heat treatment and composition ratios of raw materials used.
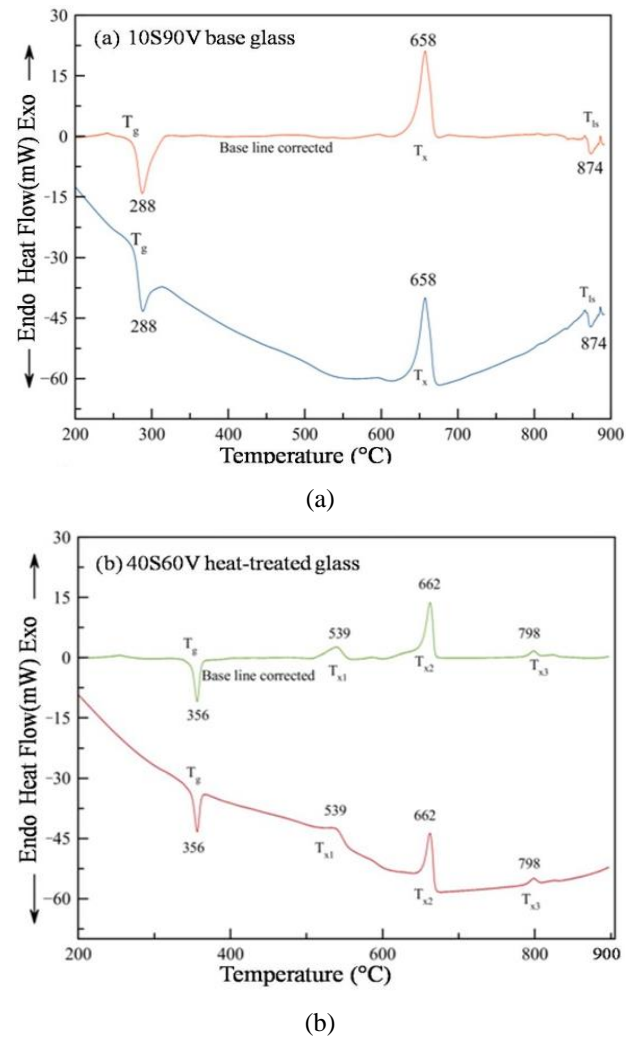

(a)

(b)

Fig. 3 DTA curves of (a) 10S90V base glass specimen and (b) 40S60V heat-treated sample.

3.3 DTA Analysis of Silicovanadate Glasses

Fig. 3 reveals the Differential Thermal Analysis (DTA) curves of 10S90V base and 40S60V heat-treated glass. The DTA traces for two glass samples are recorded in the temperature range of 30 to 900 °C, but the curves are presented from 200 to 900 °C. For 10S90V base glass, the glass transition temperature, T_g(288 °C), crystallization temperature, T_x(658 °C), and liquidus temperature T_{ls}(874 °C) are recorded. The endothermic

characteristics of the specimen are used to determine the T_g and T_{ls} while exothermic characteristics give T_x. For this composition 10S90V, the curve represents a broad exothermic peak at 658 $^\circ$C indicates T_x, and the endothermic peak at 874 $^\circ$C is a measure of the liquidus temperature (T_{ls}). Whereas, the base glass 40S60V was heat-treated at 500 °C to collect DTA data as well. In this heat-treated glass sample, the glass transition temperature is raised to 356 ºC (for endothermic reaction) with three exothermic peaks that can be visually resolved in one large and two small peaks due to the crystallization. In the sample the first peak at 539 °C, the second peak at 662 °C and the third peak at 798 °C originate due to the crystallization of various phases.

Moreover, several exothermic peaks were observed owing to the formation of various possible silicovanadate compounds such SiV_2O_7, $Si_2V_2O_6$, and $Si_2V_2O_9$ at 539 °C, 662 °C, and 798 °C respectively, as expected from X-ray diffraction data. However, the liquidus temperature (T_{sl}) could not be determined because of the poor endothermic response of the specimen. All DTA traces exhibit typical glass transitions with the inflection point between 250 to 380 $^\circ$C.
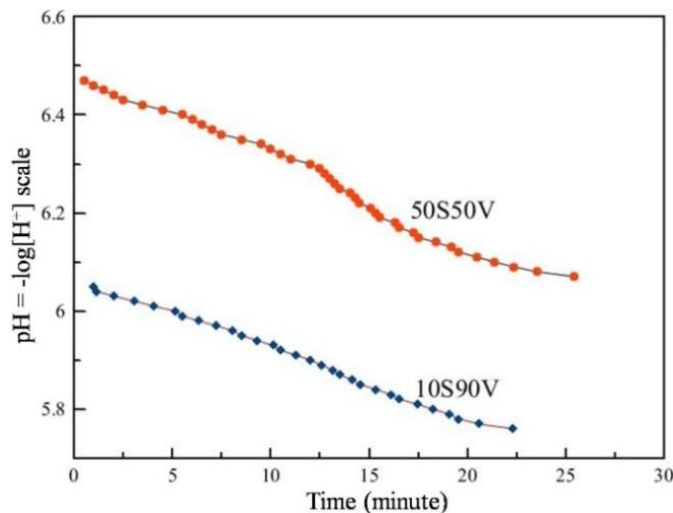

Fig. 4 Variation of pH of glass powder solution with time

3.4   pH Analysis of Silicovanadate Glasses

The pH measurement of glass samples is related to chemical durability which is defined as the stability of specimens under chemical attack. Lack of chemical durability that changes pH is mainly occurred owing to the dissolution of constituent elements in the chemical environment. It is known that higher chemical durability lowers the leaching rate of elements. A high leaching rate (lower chemical durability) is observed for high content of vanadate in contrast to more silica content glasses. The pH of the glass powder solution of 10S90V and 50S50Vcompositions in distilled H_2O are measured for 30 minutes, shown in Fig. 4. The recorded pH of the distilled water before the experimentation was 7.02. Initially, the solution of 50S50V glass powder shows the value of pH near 6.50 as seen from the curve. It is confirmed that the solution of this glass sample is acidic because the value of pH is less than 7 as there is no alkali or alkaline elements in our synthesized products. After stirring the solution by the magnetic stirrer, the value of pH gradually decreases owing to the leaching of silica and vanadate compositions in exponential form but after approximately 30 minutes the value of pH hardly changed. On the other hand, the solution of 10S90V powder sample exhibits pH ~6.10 at the beginning which shows a more acidic nature than 6S50V glass. This means that the glass

composition 10S90V exhibits lower chemical durability than that of 50S90V composition. Therefore, due to the formation of acid in distilled water the pH of the glass solution decreases as the hydrogen ion concentration increases. However, initially, the abrupt change of pH of the specimen is observed for the surface effect of V_2O_5 but strong bulk consequence becomes prominent with time. If we carry out pH measurement for all compositions from 10S90V to 50S50V it is expected that chemical inertness (less leaching rate) will increase sequentially.
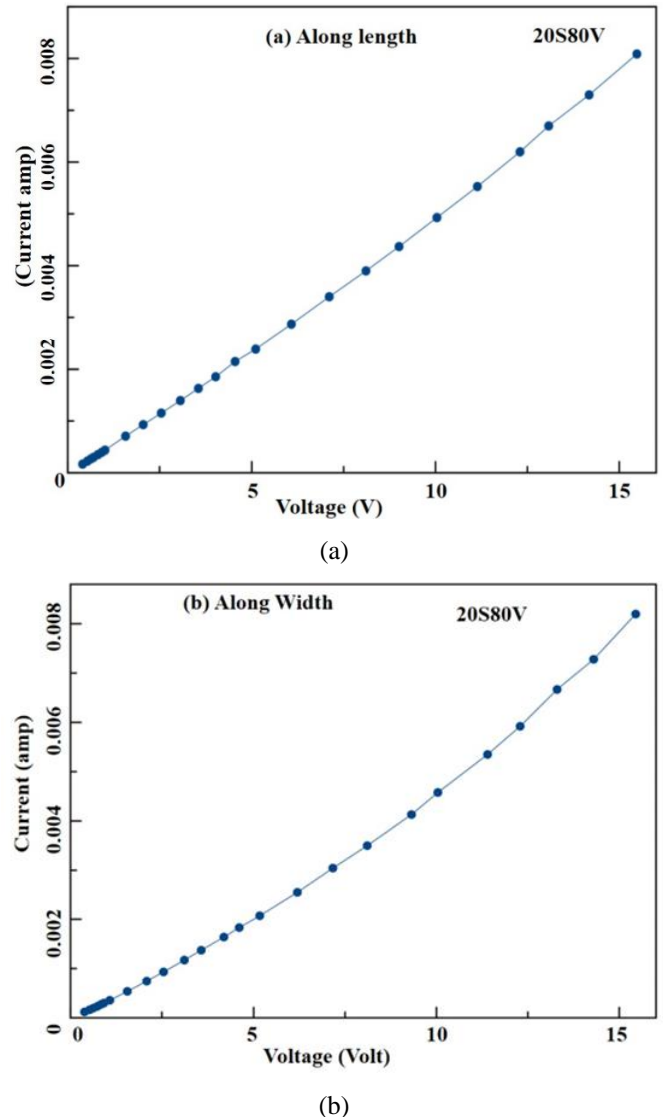

(a)

(b)

Fig. 5 $I \sim V$ Characteristic curve of the 20S80V base glass specimen along (a) length (b) width.

3.5   Vickers Hardness Analysis of Silicovanadate Glasses

Vicker hardness (H_v) data for 10S90V, 30S70V, and 40S60V base glass samples are listed in Table 3. The microhardness value of glass samples are almost comparable but vary slightly with the variation of compositions. The maximum hardness (~5.42 GPa) is observed for the glass sample 10S90V is slightly higher than two other samples (30S90V and 40S60V). However, the microhardness of glass-ceramics is mainly governed by the various cation–oxygen bond-strengths, and the glass network connectivity, and the cross-linking degree of its various segments [20]-[21],[57],[58]. The V-O-V and V=O bonds are weaker compared to Si-O-Si and O-Si-O that prevented the sequential intra-network links in the glassy

structure [46]-[48]. But the bonds of V and its local structure usually join distinct network segments, which might solidify and stiff the structure for the enhancement of H_V [59].

Table 3 Vickers hardness for 10S90V, 30S70V, and 40S60V base glass samples.

Samples	Diagonal distance (μm)		H_V (GPa)
	d_1	d_2	
10S90V	59.25(3)	56.63(6)	5.42(4)
30S70V	59.63(6)	59.69(7)	5.11(1)
40S60V	62.82(8)	57.69(7)	5.00

3.6 Electrical Conductivity (σ) of Silicovanadate Glasses

Current (Amp) versus voltage (V) characteristic curves for 20S80V specimen along the length and the width of the specimen are presented in Fig. 5(a) and 5(b) respectively. The *I~V* characteristic curves related to electrical conductivity (σ) increased gradually but not linearly with applied voltage. The deviated patterns of glass specimen from straight-line follow the relation, $I = KV^n$ where n is greater than one, which is a behavior of semiconductor. Moreover, the observed value of σ in this glass material is in the range of semi-conductivity. Moreover, Fig. 6 reveals the measured conductivity in Siemens per meter (S m^{-1}) reaches its highest value at about 440 °C. At this temperature all the impurity atoms are ionized and the number of electrons becomes maximum to get the utmost conductivity. On the other hand, the conductivity shows a sharp decreasing trend from 442 to 582 °C due to the decrease in drift mobility of electrons with the rise of temperature in this range.
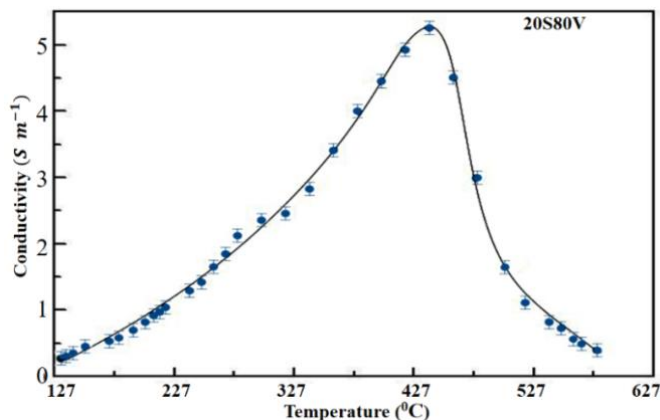

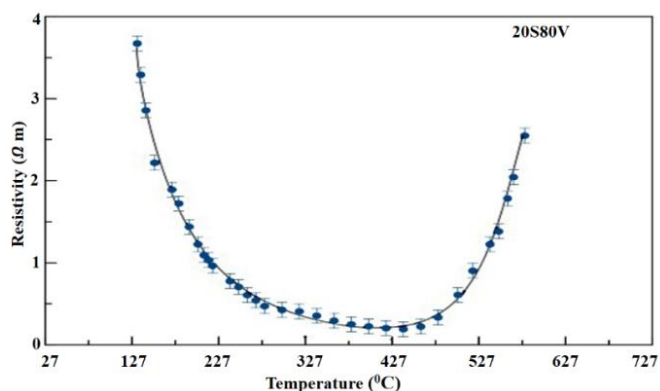Fig. 6 Variation of conductivity with a temperature of 20S80V base glass.

Fig. 7 Variation of resistivity with temperatures.

The measured resistivity of the specimen 20S80V decreases with increasing temperatures up to 427 °C is a behavior of semiconductor but metallic behavior is observed above this temperature (Fig. 7). This scenario is due to the increasing concentration of conduction electrons at elevated temperatures.

4 Conclusion

In this study, we have synthesized several silicovanadate glass samples with the variation of compositions by familiar melt quenching method. It was observed that the melting temperature of the glass samples depended on the amount of V_2O_5 present. The infrared spectra of $xSiO_2(100-x)V_2O_5$ glass system was interpreted in term of various chemical bonds. The FTIR chemical band positions in the glasses have a general tendency to shift towards the high-frequency region with the increase of V_2O_5 concentration. The FTIR spectra indicate that the glass samples contain various local structural units such as Si-O-Si, V-O-V, V-O, O-Si-O, Si–O–V, and V=O. The effect of V_2O_5 is obvious for certain bonding mechanisms where V^{5+} might play a significant role. The formation of O-H bonds expresses the hygroscopic nature of the glass which provides additional information about the structural units. The X-ray diffraction patterns of the 50S50V, 40S60V, 30S70V, 20S80V, and 10S90V base samples show an almost amorphous nature with several haloes. After heat treatment, the glasses have been crystallized with the formation of different silicovandate compounds. The characterization of samples by the DTA technique measured the T_g, T_x, and T_{ls} temperatures for glass specimens and possible randomly distributed grain of different crystalline phases. The solubility measurements of glass materials manifest the acidic nature and the pH of the sample solution decreases with the increase of V_2O_5 in the glass composition. The measured hardness of glass samples exhibits high H_V- values due to the presence of significant V-bonds in the glass structure. The higher and nonlinear conductivity patterns (I-V curve) of 20S80V glass can be considered for the semi-conductivity of the specimen which has also been supported by temperature-dependent electrical resistivity measurement data.

References

[1] Morey, G.W., 1954. Properties of glass, Monograph series (American Chemical Society), New York, Reinhold.

[2] Greer, A.L., 1997. Metallic glasses. Current Opinion in Solid State and Materials Science, 2(4), pp.412-416.

[3] Ahsan, M.R., Uddin, M.A. and Mortuza, M.G., 2005. Infrared study of the effect of P_2O_5 in the structure of lead silicate glasses.

[4] Seafriends.org.nz., 1994, Retrieved 2012, Mining the sea sand. Website: *http://www.seafriends.org.nz/oceano/seasand.htm*

[5] Sharma, B.K., 1991. Industrial chemistry. *Krishna Prakashan Media*.

[6] ElBatal, F.H., Marzouk, S.Y., Nada, N. and Desouky, S.M., 2007. Gamma-ray interaction with copper-doped bismuth–borate glasses. *Physica B: Condensed Matter*, 391(1), pp.88-97.

[7] Pönitzsch, A., Nofz, M., Wondraczek, L. and Deubener, J., 2016. Bulk elastic properties, hardness and fatigue of calcium aluminosilicate glasses in the intermediate-silica range. *Journal of Non-Crystalline Solids*, 434, pp.1-12.

[8] Sindhu, S., Sanghi, S., Agarwal, A., Kishore, N. and Seth, V.P., 2007. Effect of V_2O_5 on structure and electrical properties of zinc borate glasses. *Journal of Alloys and Compounds*, 428(1-2), pp.206-213.

[9] Singh, G.P., Kaur, P., Kaur, S. and Singh, D.P., 2011. Role of V_2O_5 in structural properties of V_2O_5-MnO_2-PbO-B_2O_3 glasses. *Materials Physics and Mechanics*, 12, pp.58-63.

[10] Seshasayee, M. and Muruganandam, K., 1998. Molecular dynamics study of V_2O_5 glass. *Solid State Communications*, 105(4), pp.243-246.

[11] Mott, N.F., 1968. Conduction in glasses containing transition metal ions. *Journal of Non-Crystalline Solids*, 1(1), pp.1-17.

[12] John, V., 1992. Introduction to engineering materials. 3rd Edition, *Macmillan Education Ltd.*

[13] Dekker, A. J., 1995. Solid-state physics, *Macmillan India Limited, New Delhi*, 110064.

[14] Cicconi, M.R., Lu, Z., Uesbeck, T., van Wüllen, L., Brauer, D.S. and De Ligny, D., 2020. Influence of Vanadium on optical and mechanical properties of aluminosilicate glasses. *Frontiers in Materials*, 7, p.161.

[15] Lewis, C.E., 1959. The biological effects of vanadium: II. The signs and symptoms of occupational vanadium exposure. *Journal of Occupational and Environmental Medicine*, 1(10), p.572.

[16] Kumar, V., Pandey, O.P. and Singh, K., 2010. Structural and optical properties of barium borosilicate glasses. *Physica B: Condensed Matter*, 405(1), pp.204-207.

[17] Limbach, R., Rodrigues, B.P. and Wondraczek, L., 2014. Strain-rate sensitivity of glasses. *Journal of Non-crystalline Solids*, 404, pp.124-134.

[18] Stevensson, B. and Edén, M., 2013. Structural rationalization of the microhardness trends of rare-earth aluminosilicate glasses: interplay between the RE3+ field-strength and the aluminum coordinations. *Journal of Non-Crystalline Solids*, 378, pp.163-167.

[19] Becher, P.F., Waters, S.B., Westmoreland, C.G. and Riester, L., 2002. Compositional effects on the properties of Si-Al-RE-based oxynitride glasses (RE= La, Nd, Gd, Y, or Lu). *Journal of the American Ceramic Society*, 85(4), pp.897-902.

[20] Rouxel, T., 2007. Elastic properties and short-to medium-range order in glasses. *Journal of the American Ceramic Society*, 90(10), pp.3019-3039.

[21] Smedskjaer, M.M., Jensen, M. and Yue, Y., 2010. Effect of thermal history and chemical composition on hardness of silicate glasses. *Journal of Non-crystalline Solids*, 356(18-19), pp.893-897.

[22] Zheng, Q., Potuzak, M., Mauro, J.C., Smedskjaer, M.M., Youngman, R.E. and Yue, Y., 2012. Composition–structure–property relationships in boroaluminosilicate glasses. *Journal of Non-crystalline Solids*, 358(6-7), pp.993-1002.

[23] Seshasayee, M. and Muruganandam, K., 1998. Molecular dynamics study of V2O5 glass. *Solid State Communications*, 105(4), pp.243-246.

[24] Kubuki, S., Matsuda, K., Akiyama, K., Homonnay, Z., Sinkó, K., Kuzmann, E. and Nishida, T., 2013. Enhancement of electrical conductivity and chemical durability of 20R2O• 10Fe2O3• xWO3•(70− x) V2O5 glass (R= Na, K) caused by structural relaxation. *Journal of Non-crystalline Solids*, 378, pp.227-233.

[25] Ghosh, A. and Chakravorty, D., 1993. Electrical conduction in some sol-gel silicate glasses. *Physical Review B*, 48(8), p.5167.

[26] Ghosh, A., 1990. Ac conduction in iron bismuthate glassy semiconductors. *Physical Review B*, 42(2), p.1388.

[27] Dutta, D. and Ghosh, A., 2005. Dynamics of Ag+ ions in binary tellurite glasses. *Physical Review B*, 72(2), p.024201.

[28] Striepe, S., Da, N., Deubener, J. and Wondraczek, L., 2012. Micromechanical properties of (Na, Zn)-sulfophosphate glasses. *Journal of Non-crystalline Solids*, 358(6-7), pp.1032-1037.

[29] Striepe, S., Smedskjaer, M.M., Deubener, J., Bauer, U., Behrens, H., Potuzak, M., Youngman, R.E., Mauro, J.C. and Yue, Y., 2013. Elastic and micromechanical properties of isostatically compressed soda–lime–borate glasses. *Journal of Non-crystalline Solids*, 364, pp.44-52.

[30] Krishna Mohan, N., Sahaya Baskaran, G. and Veeraiah, N., 2006. Dielectric and spectroscopic properties of PbO–Nb2O5–P2O5: V2O5 glass system. *Physica Status Solidi (a)*, 203(8), pp.2083-2102.

[31] Subbalakshmi, P., Sastry, P.S. and Veeraiah, N., 2001. Dielectric relaxation and ac conduction phenomena in PbO–WO3–P2O5 glass system. *Physics and Chemistry of Glasses*, 42(4-5), pp.307-314.

[32] Iordanova, R., Dimitrov, V., Dimitriev, Y. and Klissurski, D., 1994. Glass formation and structure of glasses in the V2O5-MoO3-Bi2O3 system. *Journal of Non-crystalline Solids*, 180(1), pp.58-65.

[33] Iordanova, R., Dimitriev, Y., Dimitrov, V., Kassabov, S. and Klissurski, D., 1996. Glass formation and structure in the V2O5-Bi2O3-Fe2O3 glasses. *Journal of Non-crystalline Solids*, 204(2), pp.141-150.

[34] Merzbacher, C.I. and White, W.B., 1991. The structure of alkaline earth aluminosilicate glasses as determined by vibrational spectroscopy. *Journal of Non-Crystalline Solids*, 130(1), pp.18-34.

[35] Wan, J., Cheng, J. and Lu, P., 2008. The coordination state of B and Al of borosilicate glass by IR spectra. *Journal of Wuhan University of Technology-Mater. Sci. Ed.*, 23(3), pp.419-421.

[36] Kohli, J.T., Condrate, R.A. and Shelby, J.R., 1993. Raman and infrared spectra of rare earth aluminosilicate glasses. *Physics and Chemistry of Glasses*, 34(3), pp.81-87.

[37] Hayri, E.A., Greenblatt, M., Bruna, P. and Gerhardt, R., 1989. Na2O-P2O5-SiO2 gels: Preparation and characterization. *Journal of Non-crystalline Solids*, 111(2-3), pp.167-172.

[38] Khalifa, F.A., El Hadi, Z.A., El-Keshen, A.A. and Moustaffa, F.A., 1996. Synthesis and infrared spectra of high lead silicate glasses with di-, tri-or tetravalent cations: A structure correlation. *Indian Journal of Pure & Applied Physics*, 34(4), pp.201-210.

[39] Rada, S., Neumann, M. and Culea, E., 2010. Experimental and theoretical investigations on the structure of the lead–vanadate–tellurate unconventional glasses. *Solid State Ionics*, 181(25-26), pp.1164-1169.

[40] Rada, S., Ristoiu, T., Rada, M., Dan, V., Coroiu, I., Barlea, M., Rusu, T. and Culea, E., 2010. Towards understanding of the photosensitive properties in lead–vanadate–tellurate unconventional glasses. *Materials Research Bulletin*, 45(11), pp.1598-1602.

[41] Rada, M., Rus, L., Rada, S., Pascuta, P., Stan, S., Dura, N., Rusu, T. and Culea, E., 2015. Role of vanadium ions on structural, optical and electrochemical properties of the vanadate-lead glasses. *Journal of Non-Crystalline Solids*, 414, pp.59-65.

[42] Gandhi, Y., Venkatramaiah, N., Kumar, V.R. and Veeraiah, N., 2009. Spectroscopic and dielectric properties of ZnF2–As2O3–TeO2 glass system doped with V2O5. *Physica B: Condensed Matter*, 404(8-11), pp.1450-1464.

[43] El-Bata, H.A., Ghoheim, K.A., Abd El-shafi, N. and Azooz, M.A., 2000. Infrared spectra and crystallization of some Li2O-SiO2 glasses and the effect of CaO, Al2O3 and K2O additives. *Indian Journal of Pure & Applied Physics*, 38(2), pp.101-109.

[44] Dimitrov, V., Dimitriev, Y. and Montenero, A., 1994. IR spectra and structure of V2O5-GeO2-Bi2O3 glasses. *Journal of Non-Crystalline Solids*, 180(1), pp.51-57.

[45] Srikumar, T., Rao, C.S., Gandhi, Y., Venkatramaiah, N., Ravikumar, V. and Veeraiah, N., 2011. Microstructural, dielectric and spectroscopic properties of Li2O–Nb2O5–ZrO2–SiO2 glass system crystallized with V2O5. *Journal of Physics and Chemistry of Solids*, 72(3), pp.190-200.

[46] Rao, P.T. and Vasundhara, B., 2015. Thermal and FT-IR Properties of Semiconducting SnO 2-PbO-V 2 O 5 Glass System. *New Journal of Glass and Ceramics*, 5(03), p.53.

[47] Wang, D.S. and Pantano, C.G., 1992. Structural characterization of CaO-B2O3-Al2O3-SiO2 xerogels and glasses. *Journal of Non-crystalline Solids*, 142, pp.225-233.

[48] King, P.L., Ramsey, M.S., McMillan, P.F., and Swayze, G.A.. 2004. Infrared Spectroscopy in Geochemistry, Exploration Geochemistry and Remote Sensing. *Mineral. Assoc. Canada Short Course Series*, 33, pp.57-91.

[49] Wong, J., 1976. Vibrational spectra of vapor-deposited binary phosphosilicate glasses. *Journal of Non-Crystalline Solids*, 20(1), pp.83-100.

[50] King, P.L., Ramsey, M.S., McMillan, P.F., and Swayze, G.A.. 2004. Infrared Spectroscopy in Geochemistry, Exploration Geochemistry and Remote Sensing. *Mineral. Assoc. Canada Short Course Series*, 33, pp.93-133.

[51] Ahsan, M.R. and Mortuza, M.G., 2005. Infrared spectra of xCaO (1− x− z) SiO2zP2O5 glasses. *Journal of Non-Crystalline Solids*, 351(27-29), pp.2333-2340.

[52] Chen, A. and James, P.F., 1988. Amorphous phase separation and crystallization in a lithium silicate glass prepared by the sol-gel method. *Journal of Non-crystalline Solids*, 100(1-3), pp.353-358.

[53] Rao, N.S., Purnima, M., Bale, S., Kumar, K.S. and Rahman, S., 2006. Spectroscopic investigations of Cu2+ in Li2O-Na2O-B2O3-Bi2O3 glasses. *Bulletin of Materials Science*, 29(4), pp.365-370.

[54] Mandal, S. and Hazra, S., 2000. Structural and physical properties of Fe2O3-doped lead vanadate glass. *Journal of Materials Research*, 15(1), pp.218-221.

[55] Higazy, A.A. and Bridge, B., 1985. Infrared spectra of the vitreous system Co 3 O 4-P 2 O 5 and their interpretation. *Journal of Materials Science*, 20(7), pp.2345-2358.

[56] Innocenzi, P., 2003. Infrared spectroscopy of sol–gel derived silica-based films: a spectra-microstructure overview. *Journal of Non-crystalline Solids*, 316(2-3), pp.309-319.

[57] Lofaj, F., Satet, R., Hoffmann, M.J. and de Arellano Lopez, A.R., 2004. Thermal expansion and glass transition temperature of the rare-earth doped oxynitride glasses. *Journal of the European Ceramic Society*, 24(12), pp.3377-3385.

[58] Hanifi, A.R., Genson, A., Pomeroy, M.J. and Hampshire, S., 2012. Independent but additive effects of fluorine and nitrogen substitution on properties of a calcium aluminosilicate glass. *Journal of the American Ceramic Society*, 95(2), pp.600-606.

[59] Iftekhar, S., Pahari, B., Okhotnikov, K., Jaworski, A., Stevensson, B., Grins, J. and Edén, M., 2012. Properties and structures of RE2O3–Al2O3–SiO2 (RE= Y, Lu) glasses probed by molecular dynamics simulations and solid-state NMR: the roles of aluminum and rare-earth ions for dictating the microhardness. *The Journal of Physical Chemistry C*, 116(34), pp.18394-18406.
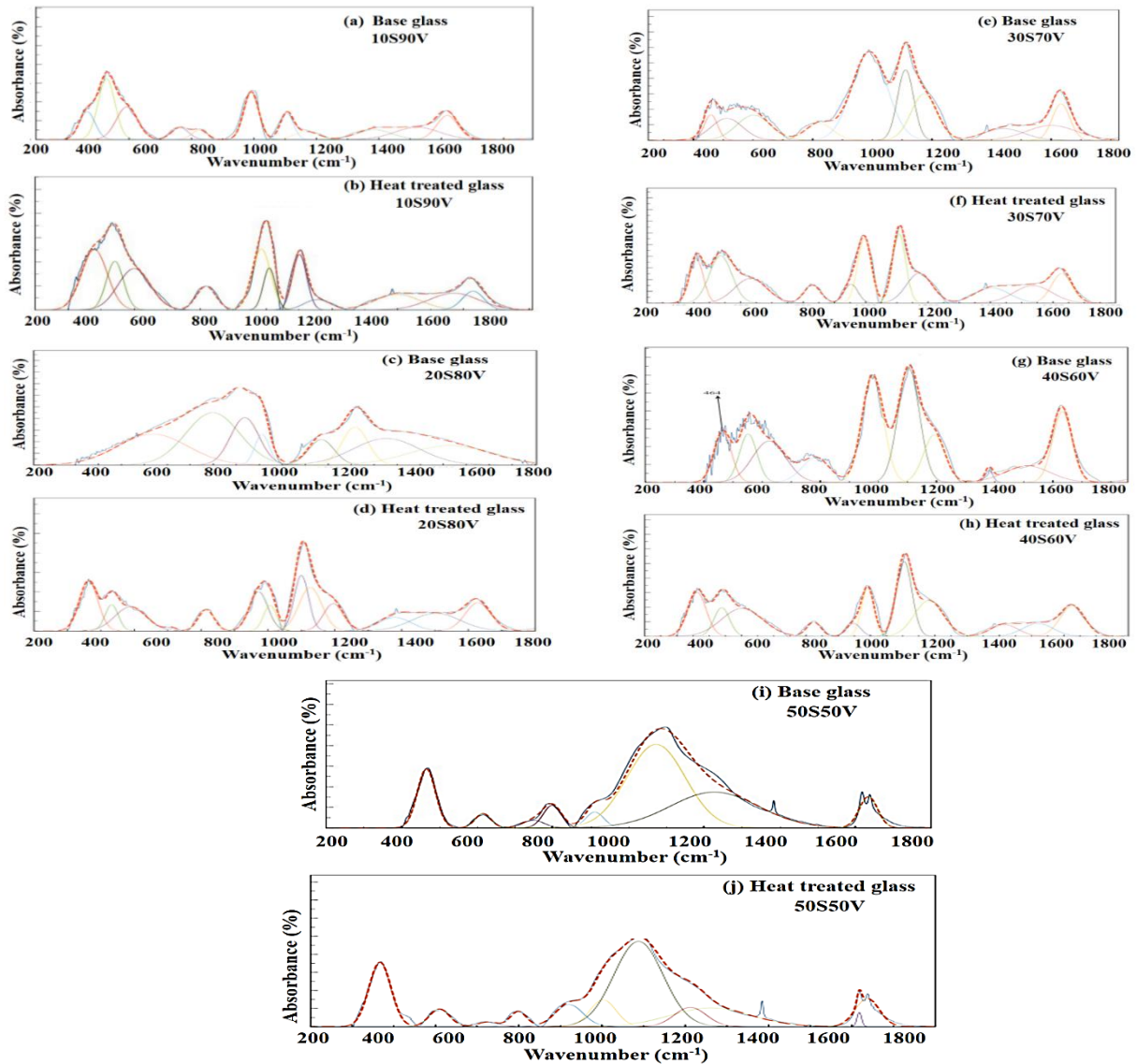
Appendix A

Fig. A1 (a), (b), (c), (d), (e), (f), (g), (h), (i) and (j) show the deconvoluted spectra of $xSiO_2(100-x)V_2O_5$ system base and heat treated glasses with x = 10, 20, 30, 40 and 50 mol % respectively.
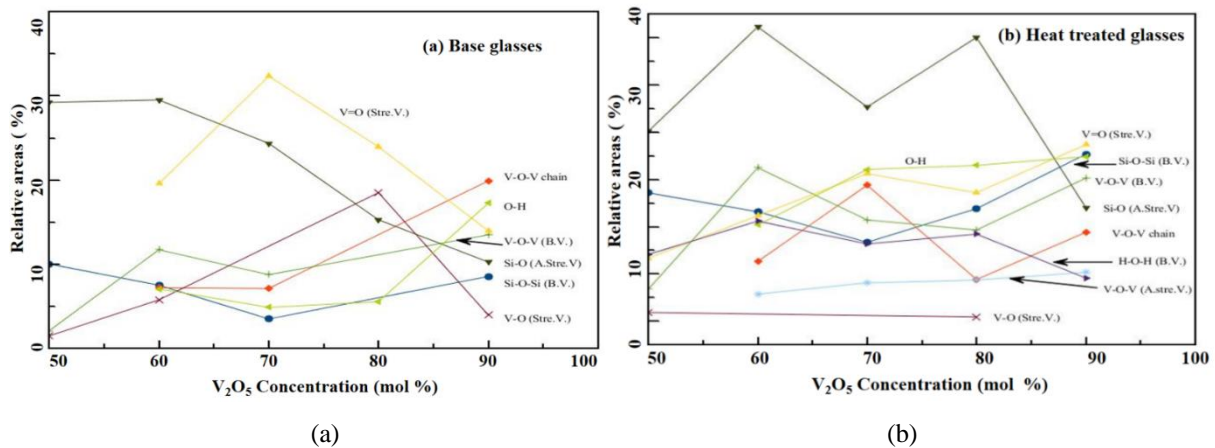

Fig. A2 (a) and (b) Relative areas of the chemical bonds as a function of V_2O_5 Concentration in mol% of $xSiO_2$ $(100-x)V_2O_5$ base and heat treated glasses respectively.